



**Ultrahigh-Q microcavity photonics
and optomechanical cooling**

Yun-Feng Xiao (肖云峰)

State Key Laboratory for Mesoscopic Physics,
Peking University, Beijing 100871, P. R. China
北京大学物理学院现代光学所
人工微结构和介观物理国家重点实验室
北京量子物质科学协同创新中心

Email: yfxiao@pku.edu.cn Tel: (86)10-62765512

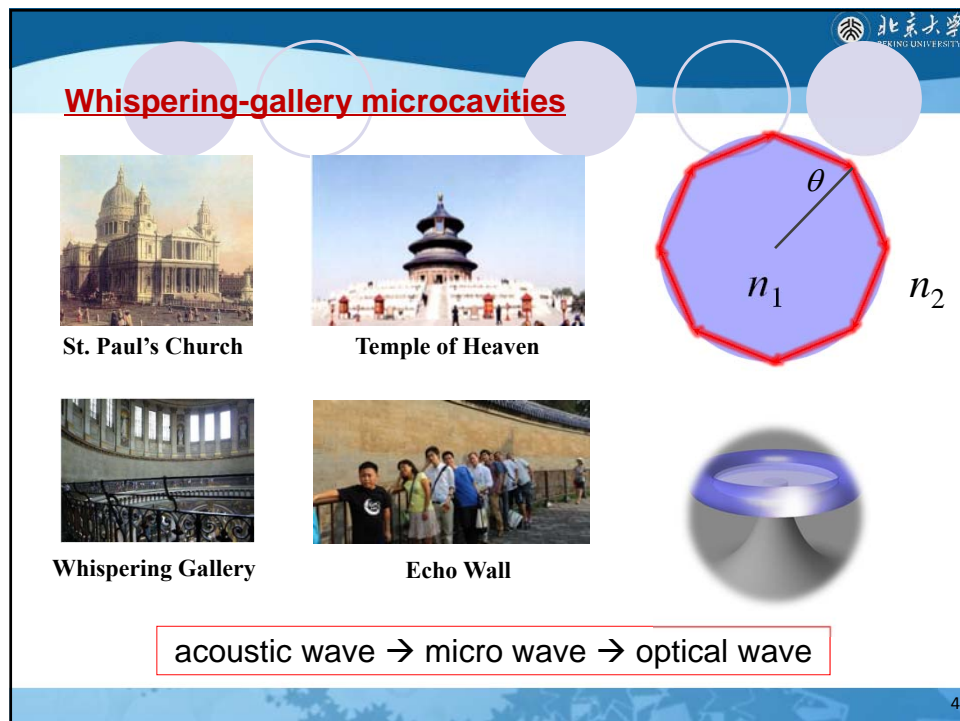
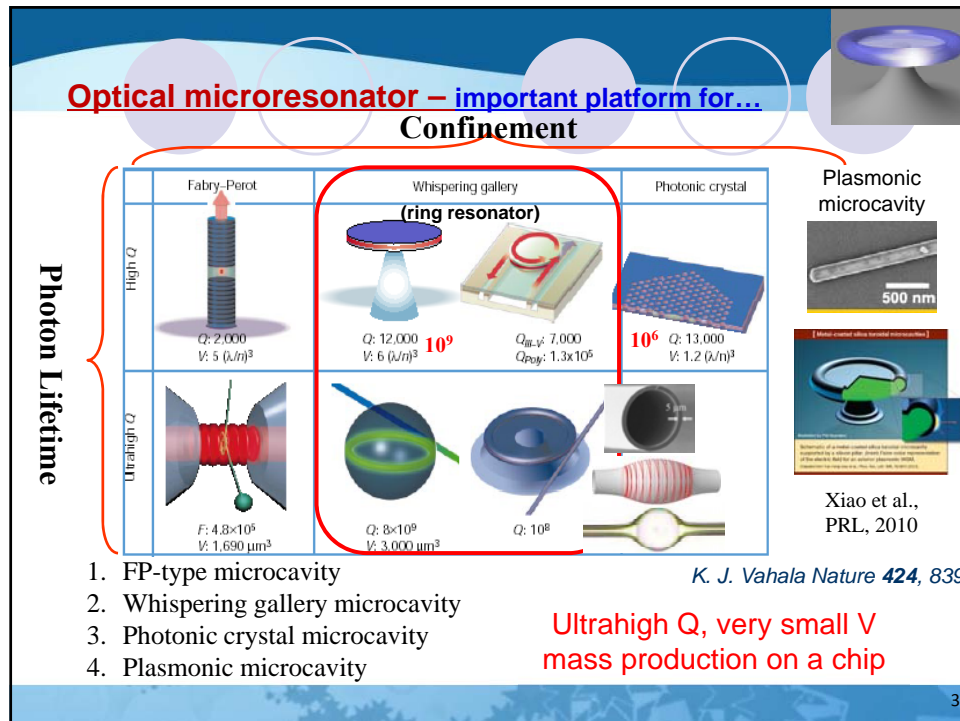
清华大学高等研究院 2015年3月11日

Microcavity photonics and quantum optics group@PKU
URL: www.phy.pku.edu.cn/~yfxiao/



Light-matter interaction plays the central role in both fundamental optical physics and applied photonics, ranging from quantum light source to functional photonic device.

2



Optical WGMs in liquid and silica microspheres

Early study: liquid droplets From liquid to solid state

many phenomena, e.g., nonlinear optical process but, suffered from evaporation

- C. G. B. Garrett, W. Kaiser, and W. L. Bond, *Phys. Rev.* 124, 1807 (1961).
- A. Ashkin and J. M. Dziedzic, *Phys. Rev. Lett.* 38, 1351 (1977).
- P. Chylek, J. T. Kiehl, and M. K. W. Ko, *Phys. Rev. A* 18, 2229 (1978).
- V. B. Braginsky, M. L. Gorodetsky, and V. S. Ilchenko, *Phys. Lett. A* 137, 393 (1989).
- M. C. Kuzyk and H. Wang, *SPIE Newsroom*. DOI: 10.1117/2.1201208.004434

5

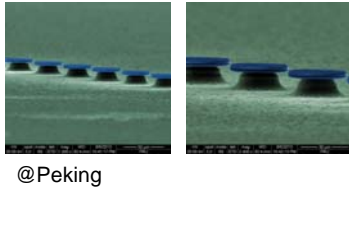
WGMs in silica microdisk and microtoroid on a chip

S. L. McCall et al., *Appl. Phys. Lett.* 60, 289 (1992) Vahala Group, *Nature* 421, 925-927 (2003)

- **Microtoroid resonator fabrication**
- Photolithographically defined photo-resist disks
- Silica etching using buffered HF and PR removal leaving silica disk
- XeF₂ isotropically etch of Si and silica disk undercut
- CO₂ laser activated reflow to form microtoroid

6

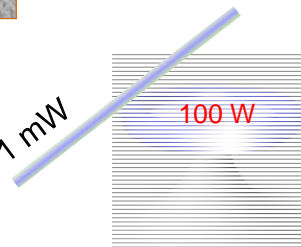
Why ultra-high-Q microcavities on a silicon chip



Diameter: 20 μm – 200 μm
Quality factor > 10^8 ,
Intracavity lifetime > 100 ns

@Peking

“Strongly enhanced light-matter interaction”



$P_{\text{in}} = 1 \text{ mW} \rightarrow$
 $P_{\text{cav}} \sim 100 \text{ W}, I_{\text{cav}} > 2 \text{ GW/cm}^2,$
 $\tau \sim 100 \text{ ns} \rightarrow \# \text{ of round trip} > 10^5.$

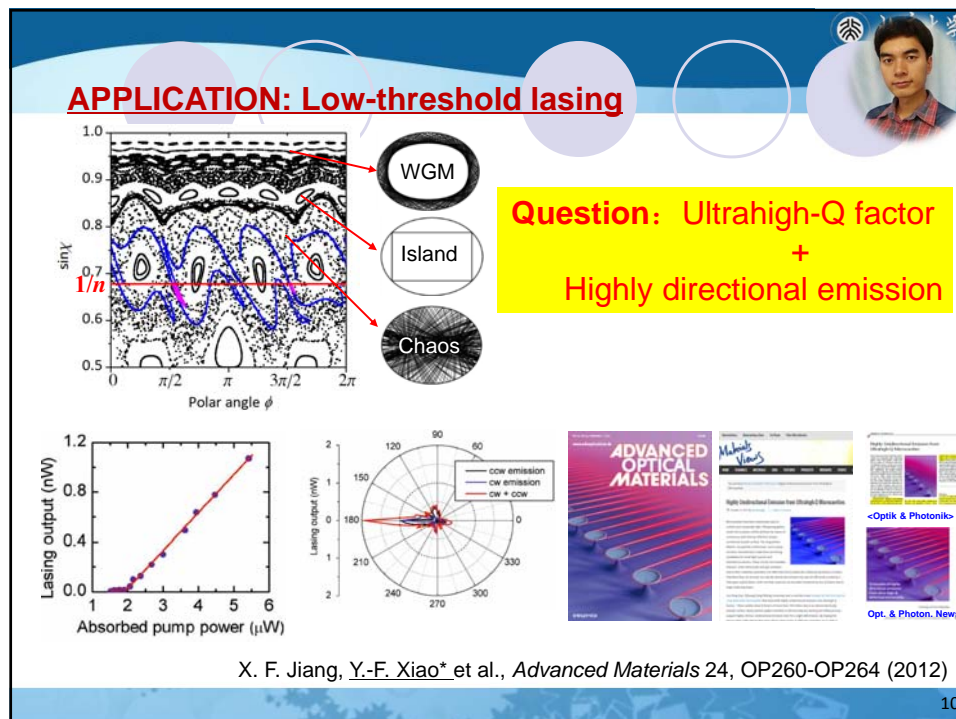
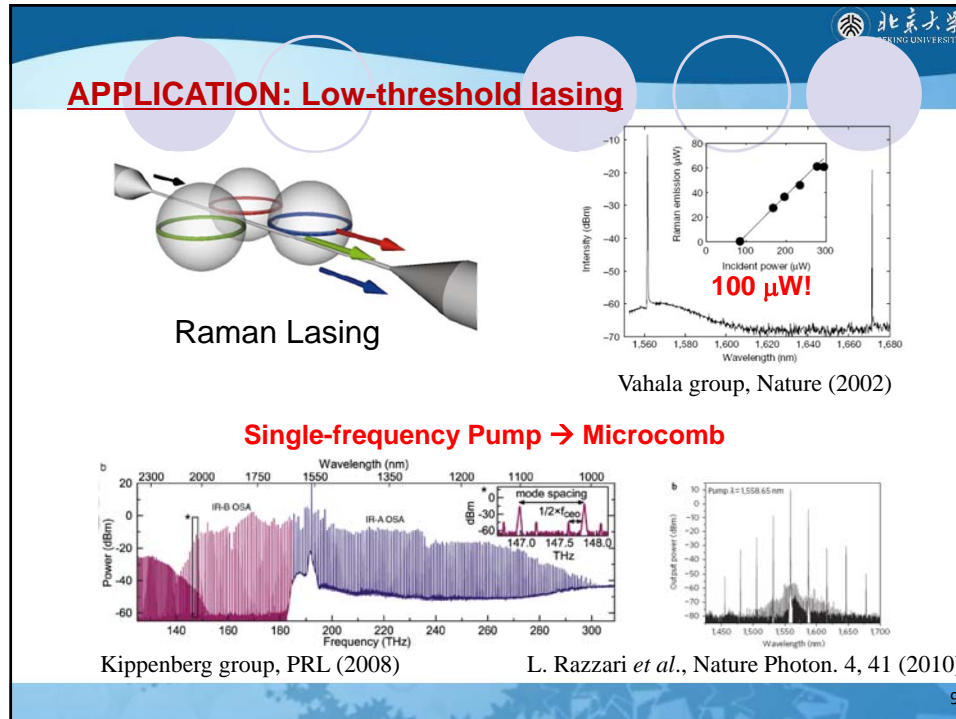
7

Our Group




Linewidth < 2 MHz
Quality factor > 2×10^8
From under coupling, critical coupling, to over coupling

8



APPLICATION: Highly sensitive optical biosensing

Mode shift

Mode splitting

Rayleigh scattering
→ mode coupling
→ mode splitting (splitting > linewidth)
(immune to thermal noise)

Thermal and probe noise

F. Vollmer & S. Arnold, Nature Methods 5, 591 (2008).
M. A. Santiago-Cordoba et al., APL 99, 073701 (2011).
J. D. Swain, J. Knittel, and W. P. Bowen, APL 99, 243109 (2011).
V. R. Dantham et al., APL 101, 043704 (2012).
Y.-F. Xiao et al., Phys. Rev. A 85, 031805(R) (2012).
V. R. Dantham et al., Nano Lett. 13, 3347 (2013).

J. Zhu et al. Nature Photonics 4, 46 (2010).
L. He et al., Nature Nanotech. 6, 428 (2011).
A. Mazzei et al. Phys. Rev. Lett. 99, 173603 (2007).
L. Chantada et al., JOSA B 25, 1312 (2008).
X. Yi, Y.-F. Xiao* et al., APL 97, 203705 (2010); PRA 83, 023802 (2011); JAP 111, 114702 (2012).

11

APPLICATION: Highly sensitive optical biosensing

Mode broadening:

- Temperature insensitive
- High sensitivity
- No requirement of ultra-high Q factors

Advanced Materials

L. Shao, X.-F. Jiang (Y.-F. Xiao*) et al., Advanced Materials 25(39), 5615 (2013)

12

APPLICATION: Highly sensitive optical biosensing

Microcavity Raman laser:

- Temperature insensitive
- Higher sensitivity than passive cavity
- No requirement of doping

Raman power (μW) vs Time (μs) plot showing oscillations.

Beat frequency (MHz) vs Time (s) plot for $r = 40 \text{ nm PS solution}$.

Inset news clipping from Phys.org: Physicists develop miniature Raman laser sensors for single nanoparticle detection.

B.-B. Li, Y.-F. Xiao* et al., PNAS 111, 14657 (2014)

13

APPLICATION: Highly sensitive optical biosensing

Nanofiber array sensor:

- No requirement of tunable laser
- Single nanoparticle response
- Large sensor area

Transmission vs Time (s) plot (b).

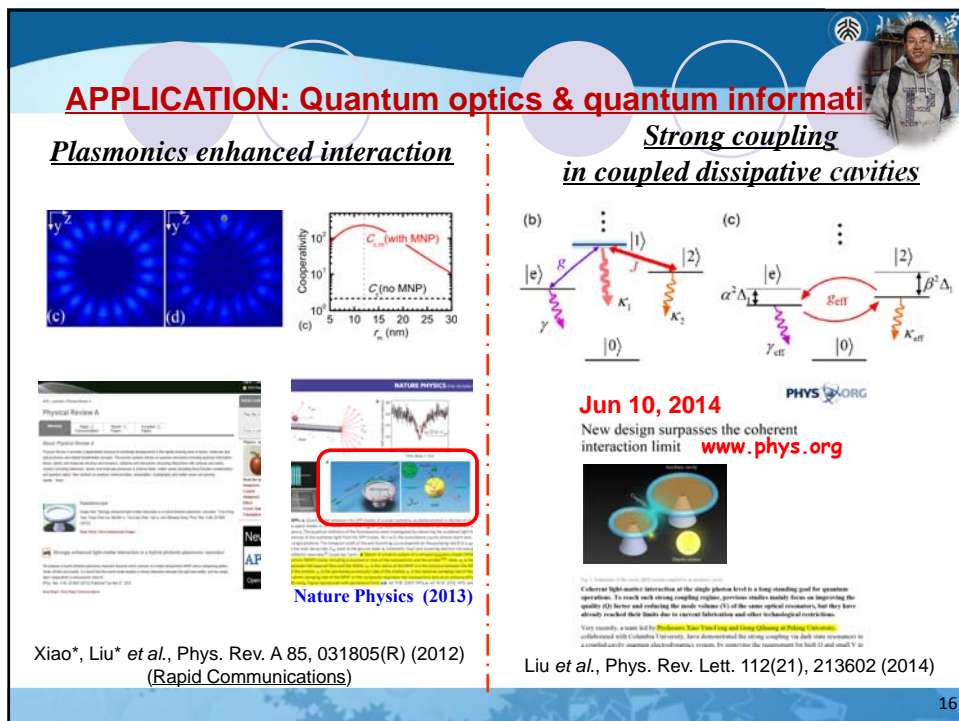
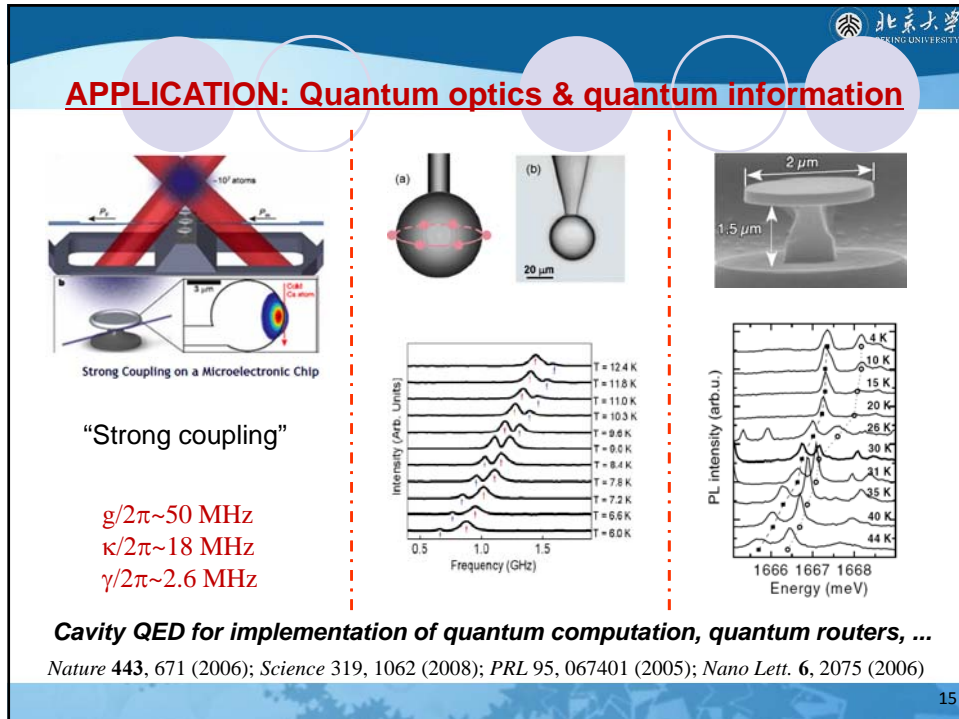
Derived sensing signal vs Counts plot (a) for $D \sim 890 \text{ nm}$ with peaks at $R=100 \text{ nm}$ and $R=170 \text{ nm}$.

Inset news clipping from MaterialsViews: Nanofiber sensor can detect and size a single nanoparticle.

Inset news clipping from Advanced Materials: Innovative Nanofiber-Array Sensor Detects and Sizes Individual Nanoparticles.

X.-C. Yu, Y.-F. Xiao* et al., Adv. Mater. 26, 7462 (2014)

14



APPLICATION: Cavity optomechanics

A schematic diagram of a microcavity containing a rotating mass. The cavity has two concentric rings. A central arrow labeled ω indicates rotation. Two other arrows labeled $\omega - \Omega$ and $\omega + \Omega$ indicate the resulting frequency detunings. The text "Vahala Group" is at the bottom.

Four 3D surface plots labeled 1, 2, 5, and 8, representing different whispering-gallery modes. Each plot shows a ring-like intensity distribution.

17

Applications of whispering gallery microcavities

Vahala, Nature, 2003

Whispering gallery

$Q: 12,000$ $V: 6 (\mu\text{m})^3$	$Q_{\text{eff},V}: 7,000$ $Q_{\text{Poly}}: 1.3 \times 10^6$

$Q: 8 \times 10^9$ $V: 3,000 \mu\text{m}^3$	

Ultrahigh Q , very small V , and mass production on a chip

Excellent platform for Fundamental physics:

- Quantum optics
- Cavity quantum electrodynamics (QED)
- Quantum information
- Quantum chaos
- Cavity quantum optomechanics**
-

Microphotonics:

- Highly sensitive bio/chemical sensing
- All-optical low-threshold switching
- On-chip microlasing (includ. Raman)
- Optical microcomb
- Optical filtering...

18

Outline

1. Introduction
2. Cooling in the strong coupling regime
 - Dynamic dissipative cooling
3. Cooling in the intermediate coupling regime
 - Room-temperature ground-state cooling
4. Summary

19

Mechanical effect of light

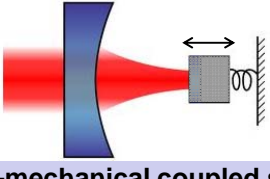
Cavity optomechanics

Astronomic scale




Comet's tail Kepler

Macro and Mesoscopic scale



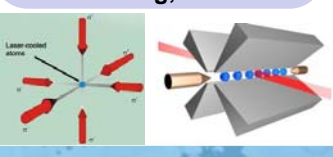
Opto-mechanical coupled system

Optical force acts on the mirror;
Mirror's motion state changes;
Cavity length changes;
Cavity field changes;

Microscopic scale



Laser cooling, Nobel 1997



20

Applications

- Fundamental studies of quantum theory
 - Macroscopic quantum state, superposition and entanglement
 - Quantum-classical boundary
- Precision measurement
 - Gravitational waves detection
 - Mass, force and displacement
- Quantum information processing platform

Kippenberg & Vahala
Science, 321, 1172 (2008)

Trapped particle
Cold atoms/BEC

Weiping Zhang group,
PRL 108, 240405 (2012)

21

WGM Cavity optomechanics

Vahala Group

1 2
5 8

22

Optomechanical coupling (dispersive)

C. K. Law et al., 1990s

System Hamiltonian

$$H = \omega_c(x)a^\dagger a + \omega_m b^\dagger b$$

The cavity resonance frequency is modulated by the mechanical motion

$$\omega_c(x) = \omega_c + x \partial \omega_c(x) / \partial x + \mathcal{O}(x)$$

$x = x_{\text{ZPF}}(b^\dagger + b)$ Zero-point fluctuation: $x_{\text{ZPF}} = \sqrt{\hbar / (2m_{\text{eff}}\omega_m)}$

$H_{\text{int}} = g a^\dagger a (b^\dagger + b)$ Optomechanical coupling:

$$H_0 = \omega_c a^\dagger a + \omega_m b^\dagger b$$

$$g = [\partial \omega_c(x) / \partial x] x_{\text{ZPF}}$$

Coherent laser input

$$H_{\text{drive}} = \Omega^* e^{i\omega_{\text{in}} t} a + \Omega e^{-i\omega_{\text{in}} t} a^\dagger \quad \Omega = \sqrt{\kappa_{\text{ex}} P / (\hbar \omega_{\text{in}})} e^{i\phi}$$

Linearization $a \rightarrow a_1 + \alpha, b \rightarrow b_1 + \beta$

$H_L = -\Delta' a_1^\dagger a_1 + \omega_m b_1^\dagger b_1 + (G a_1^\dagger + G^* a_1)(b_1 + b_1^\dagger)$

$G = \alpha g \quad \Delta' = \omega - \omega_c + 2|G|^2 / \omega_m$

23

Optomechanical coupling

Important parameters

- ω_m : mechanical frequency
- G : coupling strength
- κ : optical decay
- γ : mechanical decay
- n_{th} : thermal phonon number

Unresolved sideband regime : $\omega_m < \kappa$

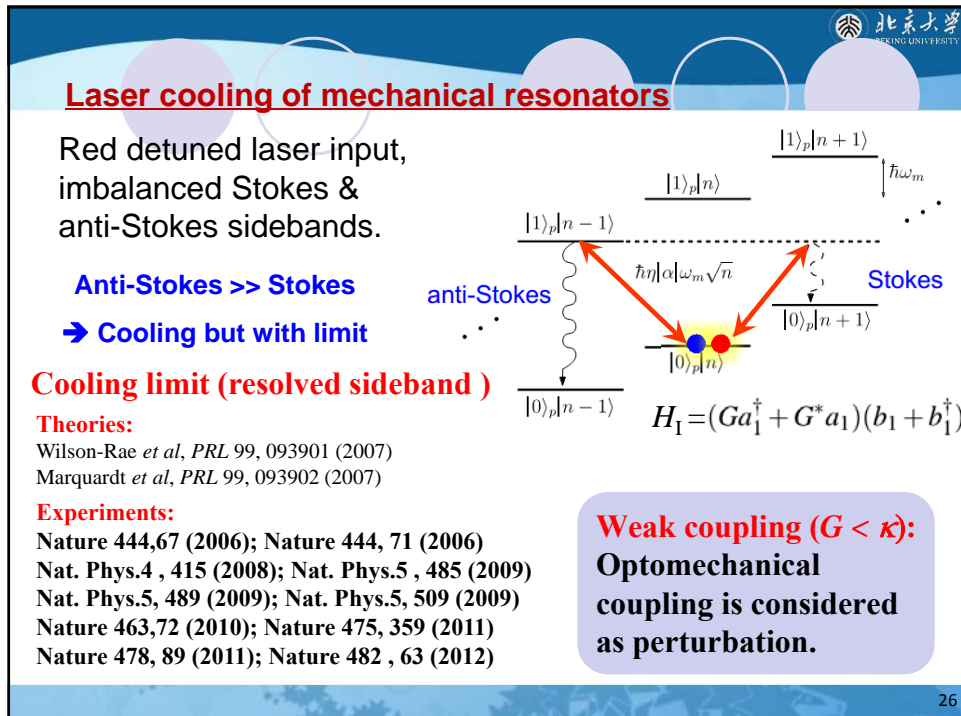
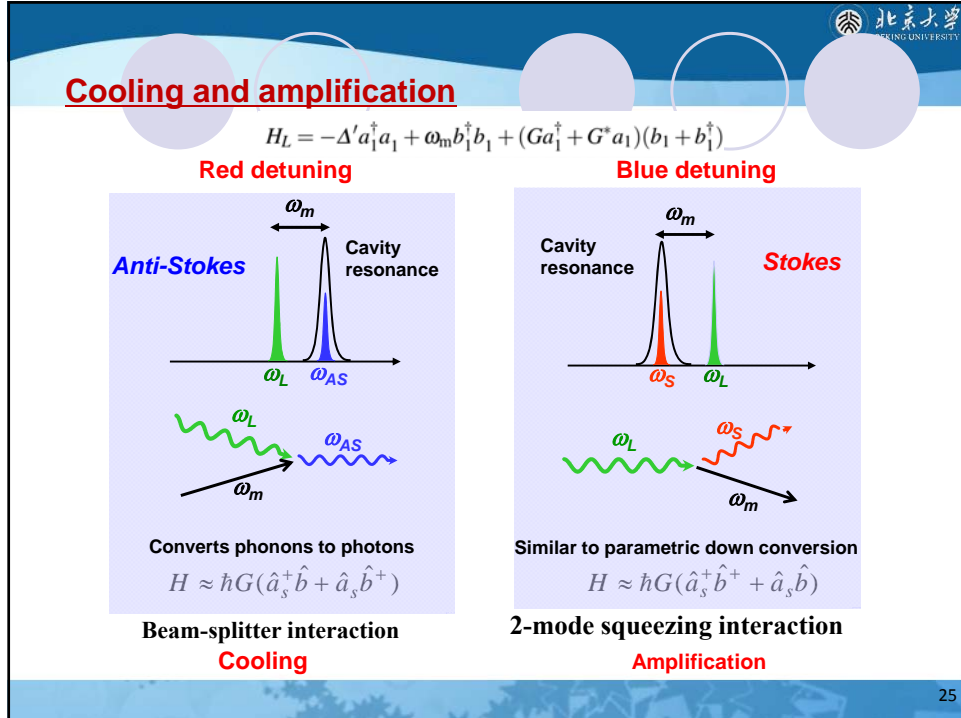
Resolved sideband regime : $\omega_m > \kappa$

Weak coupling regime: $G < \kappa$

Strong coupling regime: $G > \kappa$

ω_m

24



Cooling beyond the weak coupling regimes

From weak to intermediate or even strong coupling regime ($G > \kappa$)

Theory: Dobrindt *et al*, PRL 101, 263602 (2008);
Experiment: Verhagen *et al*, Nature (2012); Palomaki *et al*, Nature (2013).

- Important for quantum applications
- Requires non-perturbative calculation

27

Cooling beyond the weak coupling regimes

Non-perturbative approach:

$$\dot{\rho} = i[\rho, H_L] + \kappa \mathcal{D}[a_1] \rho + \gamma(n_{\text{th}} + 1) \mathcal{D}[b_1] \rho + \gamma n_{\text{th}} \mathcal{D}[b_1^\dagger] \rho$$

$$\dot{\mathbf{V}} = \mathbf{M}\mathbf{V} + \mathbf{N},$$

$$\mathbf{V} = (\bar{N}_a, \bar{N}_b, \langle a_1^\dagger b_1 \rangle, \langle a_1 b_1^\dagger \rangle, \langle a_1 b_1 \rangle, \langle a_1^\dagger b_1^\dagger \rangle, \langle a_1^2 \rangle, \langle a_1^{\dagger 2} \rangle, \langle b_1^2 \rangle, \langle b_1^{\dagger 2} \rangle)^T$$

$$\mathbf{N} = (0, \gamma n_{\text{th}}, 0, 0, -iG, iG^*, 0, 0, 0, 0)^T$$

- Valid in weak, intermediate and strong coupling regimes
- Can study dynamics behavior, in addition to steady state

Y.-C. Liu et al., PRA 89, 053821 (2014)

28

Outline

1. Introduction
2. Cooling in the strong coupling regime
 - Dynamic dissipative cooling
3. Cooling in the intermediate coupling regime
 - Room-temperature ground-state cooling
4. Summary

29

Cooling in the strong coupling regime

Time evolution of average phonon number in weak and strong coupling regimes (numerical result)

$n_{\text{th}} = 10^3, \gamma/\omega_m = 10^{-5}, \text{ and } \kappa/\omega_m = 0.05$

Characteristics of cooling in strong coupling regime

- Oscillation and cooling rate saturation
- Instantaneous-state cooling limit

30

Cooling in the strong coupling regime

Under rotating-wave approximation (RWA) $|G| \ll \omega_m$

$$\bar{N}_b^{\text{RWA}}(t) \simeq n_{\text{th}} \frac{\gamma + e^{-\frac{\kappa+\gamma}{2}t} [\kappa \cos^2(|G|t) - \gamma \sin^2(|G|t)]}{\kappa + \gamma}$$

$$n_{\text{ins}}^{\text{RWA}} \simeq \frac{\pi \gamma n_{\text{th}}}{4 |G|}$$

$n_{\text{th}} = 1000 \quad G/\omega_m = 0.1; G/\omega_m = 0.05 \quad t \sim \pi/(2G)$

Data: numerical result;
Curve: analytical result (RWA) Y.-C. Liu et al., PRA 89, 053821 (2014)

“研究热环境的影响”
 $N_b, n_{\text{ins}} \propto n_{\text{th}}$

31

Cooling in the strong coupling regime

Without RWA, $n_{\text{th}} = 0$ “研究反旋波的影响”

$$\bar{N}_b^{(0)}(t) \simeq \frac{|G|^2 [1 - e^{-\frac{\kappa+\gamma}{2}t} \cos(\omega_+ + \omega_-)t \cos(\omega_+ - \omega_-)t]}{2(\omega_m^2 - 4|G|^2)}$$

$$\omega_{\pm} = \sqrt{\omega_m^2 \pm 2|G|\omega_m}$$

Frequency matching condition:

$$(\omega_+ + \omega_-)t = p\pi, \quad p, q$$

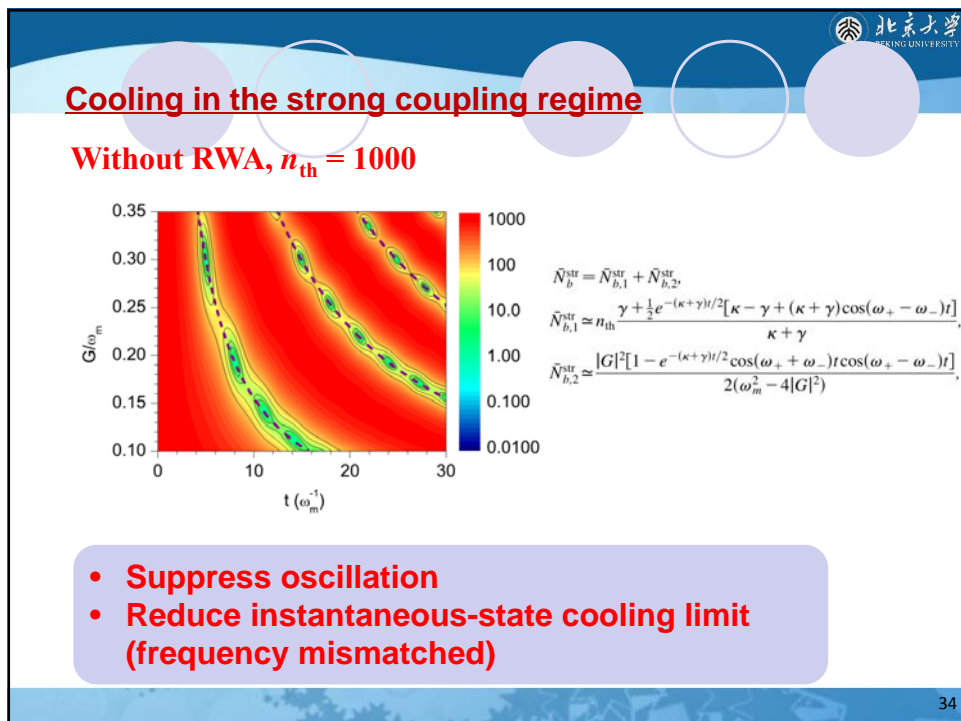
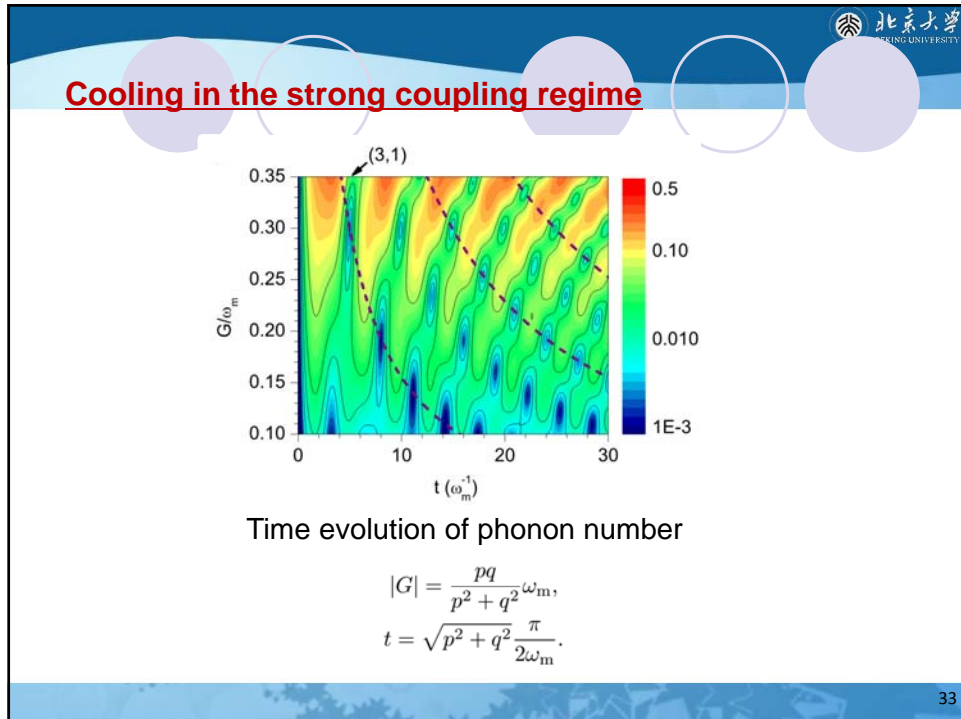
$$(\omega_+ - \omega_-)t = q\pi, \quad \text{both odd or even}$$

$|G| = \frac{pq}{p^2 + q^2}\omega_m,$

$n_{\text{ins}}^{(0)} \simeq \frac{\pi \kappa |G|}{8(\omega_m^2 - 4|G|^2)}$

$G/\omega_m = 0.3$
 $G/\omega_m = 0.35$

32



Dynamic dissipative cooling approach

Cooling processes:

- A: Energy swapping
- C: Counter-rotating-wave interaction
- E: Cavity dissipation

Heating processes:

- B: Swap heating
- D: Quantum backaction heating
- F: Thermal heating

Dissipation pulses

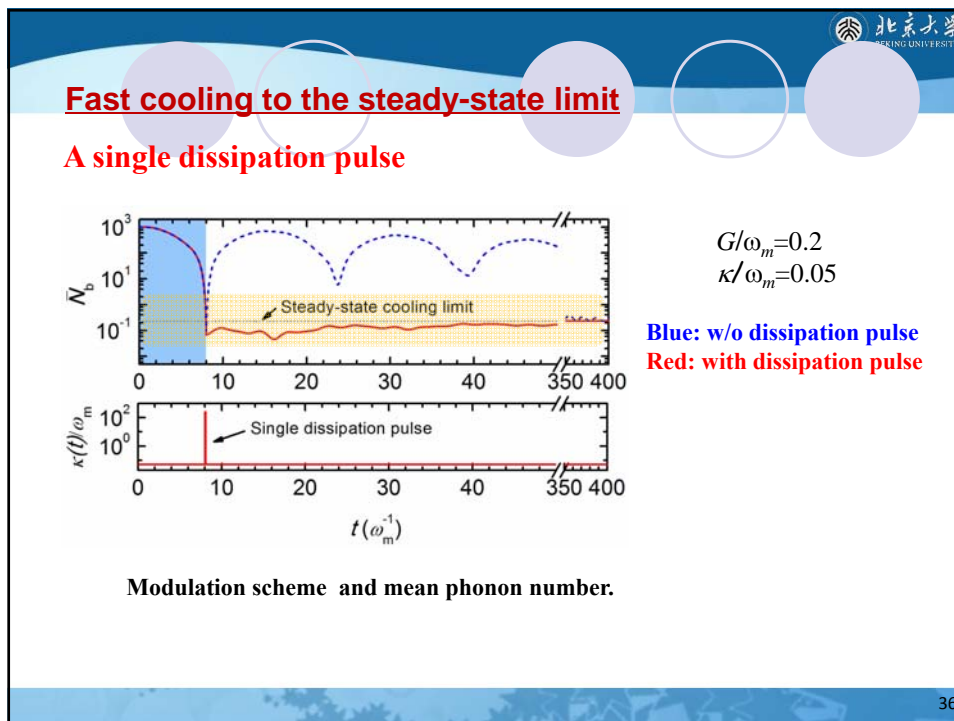
*n: photon number
m: phonon number*

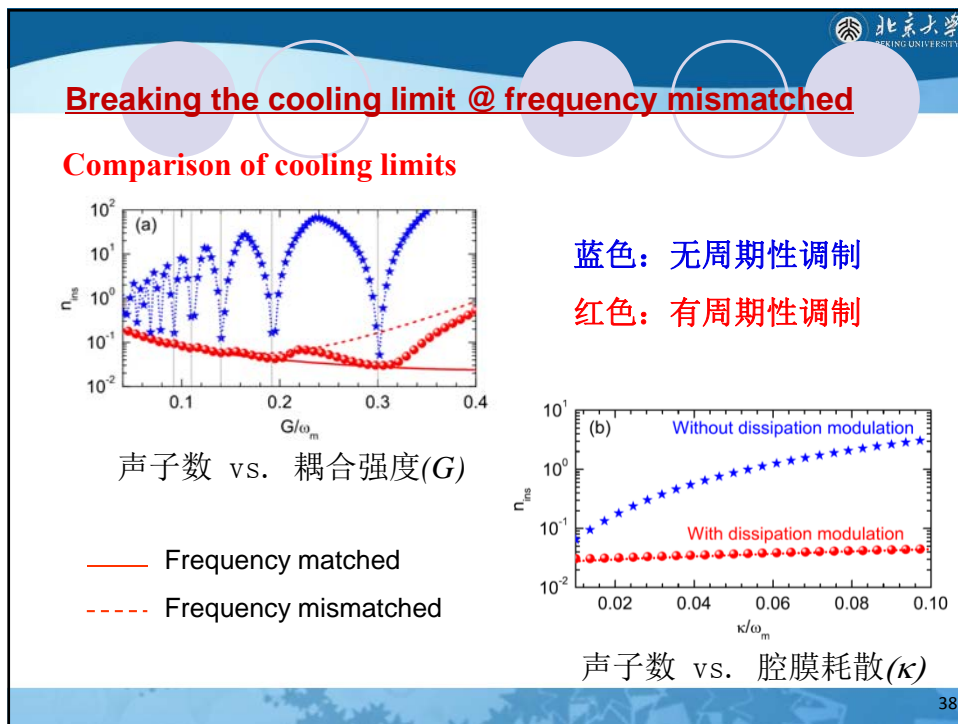
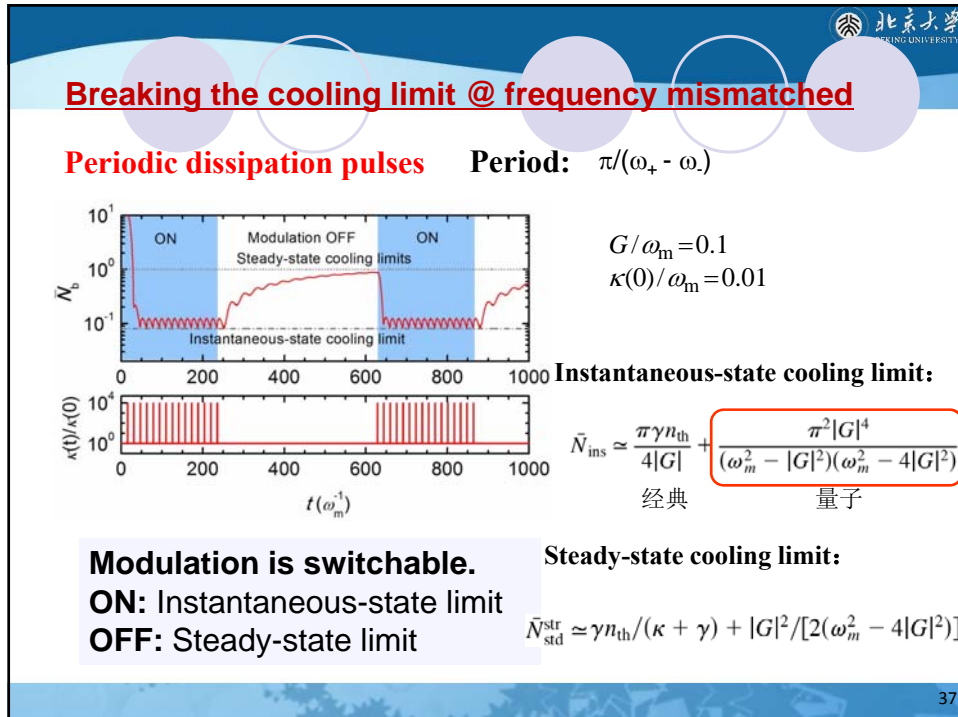
Strong coupling: E is slower than A/B .

→ **Dynamically modulate E process.**

Y.-C. Liu *et al.*, Phys. Rev. Lett. 110, 153606 (2013)

35





Experimental realization

Modulation of cavity decay rate

- **By modulating the free-carrier plasma density.**
 - The absorption is affected by injection of charge carriers into an undoped sample.
- **By using a light absorber/scatterer.**
 - The position change of a light absorber/scatterer leads to the change of the cavity dissipation by absorption of photons and Rayleigh scattering photons out of the cavity.

Q. Xu *et al.*, *Nat. Phys.* **3**, 406 (2007); K. Kondo *et al.*, *Phys. Rev. Lett.* **110**, 053902 (2013); I. Favero *et al.*, *New J. Phys.* **10**, 095006 (2008).

39

Outline

1. **Introduction**
2. **Cooling in the strong coupling regime**
 - Dynamic dissipative cooling
3. **Cooling in the intermediate coupling regime**
 - Room-temperature ground-state cooling
4. **Summary**

40

Cooling in the intermediate coupling regime

Exact results of the steady-state cooling limit:

$$n_s = n_s^{(1)} + n_s^{(0)}$$

Classical cooling limit Quantum cooling limit

Originates from the mechanical dissipation and is proportional to n_{th} *Originates from the quantum backaction and does not depend on n_{th}*

Approximate analytical results under resolved sideband limit:

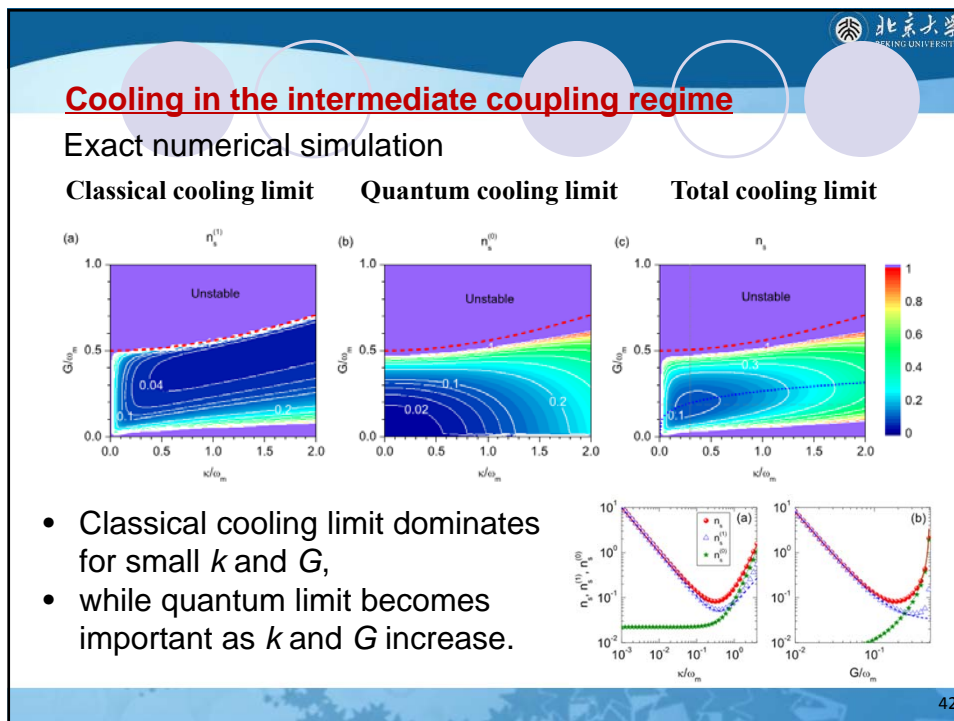
$$n_s^{(1)} |_{\Delta' = -\omega_m} \simeq \frac{4|G|^2 + \kappa^2}{4|G|^2 \kappa} \gamma n_{th},$$

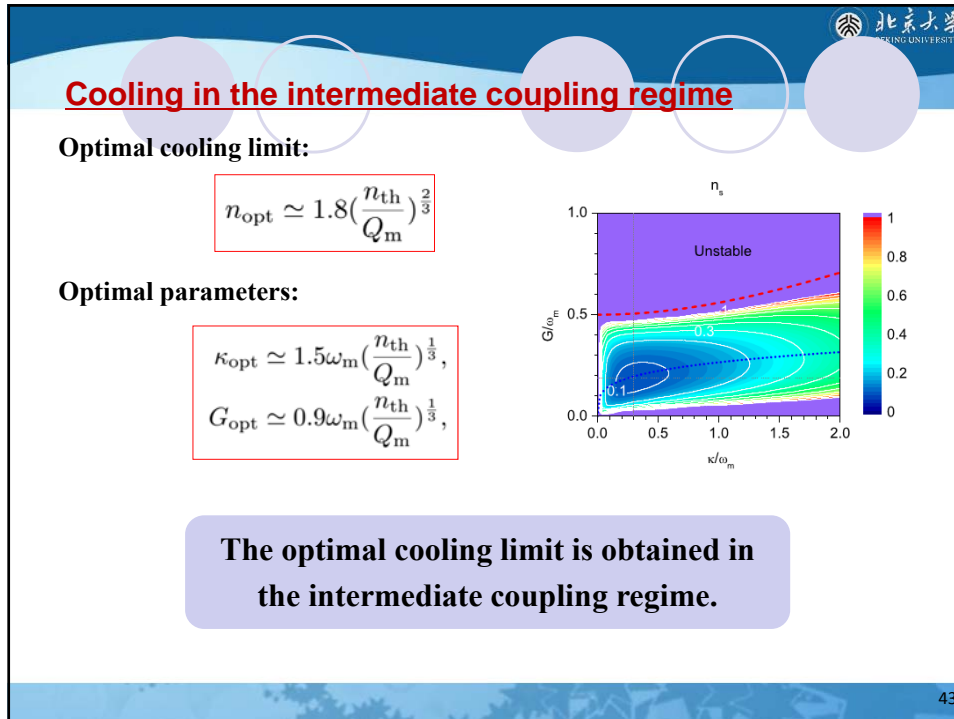
$$n_s^{(0)} |_{\Delta' = -\omega_m} \simeq \frac{\kappa^2 + 8|G|^2}{16(\omega_m^2 - 4|G|^2)}.$$

ω_m : mechanical frequency
 G : coupling strength
 κ : optical decay
 γ : mechanical decay
 n_{th} : thermal phonon number

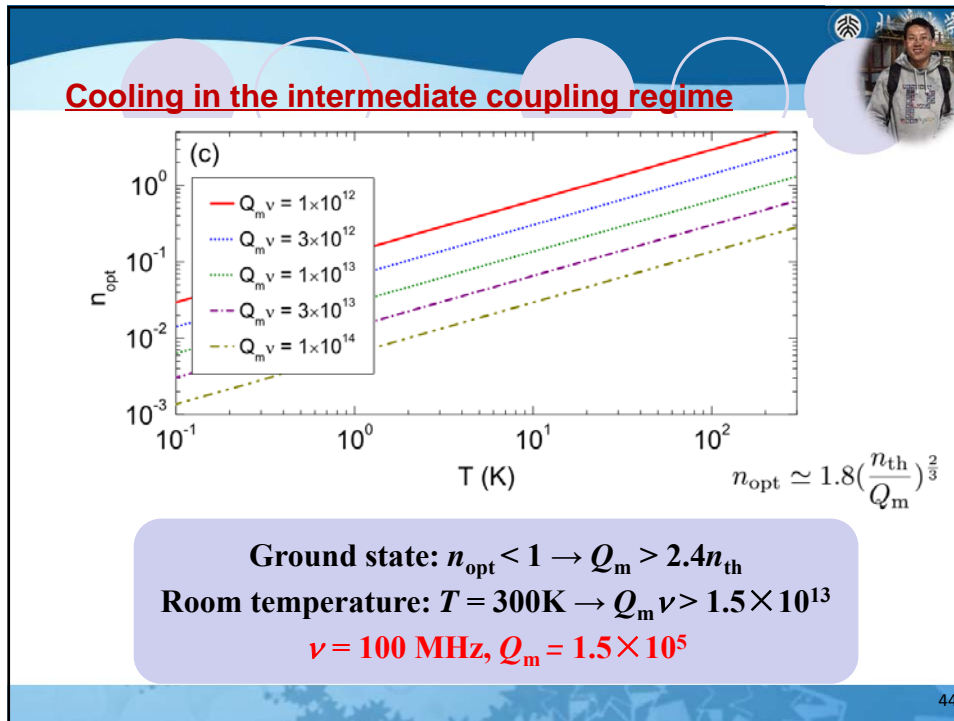
at $G \rightarrow 0$, agree to previous result (微扰) Y.-C. Liu et al., unpublished

41





43

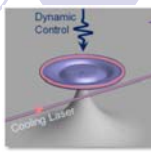


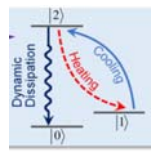
44

Summary

1. Ultra-high-Q microcavity photonics
2. Cooling in the strong coupling regime
 - Dynamic dissipative cooling
3. Cooling in the intermediate coupling regime
 - Room-temperature ground-state cooling







• Y.-C. Liu, Y.-F. Xiao* et al., PRL 112, 213602 (2014).
 • Y.-C. Liu, Y.-F. Xiao* et al., PRL 111, 083601 (2013).
 • Y.-C. Liu, Y.-F. Xiao* et al., PRL 110, 153606 (2013).
 • Y.-C. Liu, Y.-F. Xiao* et al., Science China, in press
 • Y.-C. Liu, Y.-F. Xiao* et al., PRA 89, 053821 (2014).
 • H.-K. Liu, Y.-F. Xiao* et al., PRA 88, 053850 (2013).
 • M.-Y. Yan, Y.-F. Xiao* et al., PRA 88, 023802 (2013).
 • X.-X. Ren, Y.-F. Xiao* et al., PRA 87(3), 033807 (2013).
 • H.-K. Li, Y.-F. Xiao* et al., PRA 85, 053832 (2012)
 • Y.-F. Xiao* et al., PRA 85, 031805(R) (2012). Rapid Comm.
 • Y.-C. Liu, Y.-F. Xiao* et al., PRA 84, 011805(R) (2011). Rapid Comm.
 • Y.-C. Xiao* et al., PRA 81(5), 053807 (2010).
 •

Thank you for your attention!

For more information:
 Microcavity Photonics and Quantum Optics
<http://www.phy.pku.edu.cn/~yfxiao/>




45